Multi-walled Carbon Nanotubes/Ionic Liquid Nanocomposite Modified Carbon-ceramic Electrode: Electrochemistry and Measurement of Tryptophan in the Presence of Uric Acid

Biuck Habibi*, Zahra Ayazi and Maryam Dadkhah

Electroanalytical Chemistry Laboratory, Department of Chemistry, Faculty of Sciences, Azarbaijan Shahid Madani University, Tabriz 53714-161, Iran

(Received 2 November 2016, Accepted 1 March 2017)

In the present work, an efficient modified carbon-ceramic electrode by multi-walled carbon nanotubes/ionic liquid nanocomposite (MWCNTs/IL/CCE) was prepared through a simple and repeatable procedure. The introduced modified electrode was used for the study of the electrochemical behaviour and determination of tryptophan (Trp) in the presence of uric acid (UA) using cyclic voltammetry (CV), differential pulse voltammetry (DPV) and amperometry techniques. The MWCNTs/IL/CCE exhibited high electrocatalytic activity toward the oxidation of Trp in phosphate buffer solution (pH 7.0) which led to produce an anodic peak at about 0.67 V *vs.* saturated calomel electrode. The influential parameters such as pH, amount and ratio of MWCNTs/IL in the nanocomposite modifier on the electrocatalytic activity of the MWCNTs/IL/CCE were studied and optimized. Under the optimum conditions, the anodic peak current in DPV method is linear for the Trp concentrations in the ranges of 5×10^{-7}-7×10^{-5} M with a correlation coefficient of 0.998 and detection limit of 3.2×10^{-7} M (S/N = 3). The relative standard deviation of the anodic peak current obtained for a 5.0×10^{-5} M Trp solution was 2.2% (n = 6). Finally, DPV method was applied for simultaneous determination of Trp and UA, demonstrating the applicability of the present modified electrode.

Keywords: Multi-walled carbon nanotubes, Ionic liquid, Nanocomposite, Tryptophan, Uric acid, Simultaneous determination, Modified electrode

INTRODUCTION

Tryptophan (Trp) [(2S)-2-amino-3-(1H-indol-3-yl) propanoic acid] is one of the 20 standard amino acids provided from the human diet and is necessary in the human body for normal growth in infants and nitrogen balance in adults. Additionally, it is a vital constituent of proteins and an essential amino acid prepared by human nutrition; *i.e.*, your body cannot produce it, to establish and maintain a positive nitrogen balance [1]. Due to its scarcely presence in the vegetables and also other food sources, Trp is added to dietary, food products and pharmaceutical formulas. Therefore, development of a simple, sensitive and selective method for determination of Trp in food and pharmaceutical products and also biological samples is very important. Various non-electroanalytical methods such as high-performance liquid chromatography [2-4], capillary electrophoresis [5-7], fluorometric methods [8-9], chemiluminescence [10-12] and spectrometric analysis [13, 14] have been reported for the quantification of Trp concentration in foods, pharmaceutical preparations and biological samples. Although these methods own the advantages of sensitivity and accuracy, their wide application is limited due to their high costs and complicated operations. Thus, it is necessary to develop novel strategies for the determination of Trp concentration in various samples. Electroanalytical methods owning sensitivity, accuracy, simplicity and low cost have attracted considerable attention in analytical chemistry of Trp. However, the electrochemical determination of Trp

*Corresponding author. E-mail: B. Habibi@azaruniv.ac.ir

concentration on unmodified and bare electrode is not desirable because of sluggish electron-transfer processes and high overpotential of its electrooxidation [15]. Hence, numerous research activities have been conducted to introduce efficient materials as the electrode modifier that can reduce the overpotential of Trp and improve the rate of electron-transfer processes. Recently, various modified electrodes have been utilized to analyse Trp in pharmaceutical, clinical preparations and other samples [16-25]. Uric acid (UA), [7,9-Dihydro-1*H*-purine-2,6,8(3*H*)-trione], is also a primary end product of urine metabolism existing in the blood of human body. Abnormal levels of UA exhibit symptoms of several diseases like gout, hyperuricaemia and Lesch-Nyhan syndrome. Also, the elevated UA concentration in serum causes kidney damage and cardiovascular disease. Since, Trp and UA are present in blood serum simultaneously, it is essential to develop simple and rapid electrochemical methods for determination of these biological molecules in routine analysis. In recent years, development of voltammetric sensors for simultaneous determination of such biological molecules in human fluid, food processing, pharmaceuticals, and clinical analysis has received considerable interest [15,18-20,25].

The carbon nanotubes (CNTs) and room-temperature ionic liquids (RTILs) nanocomposites, CNTs/RTILs, have received more and more attention of researchers [26-32] since Fukushima [33] found that CNTs can generate gels by simply grinding them with RTILs. It is well known that the successful combination of CNTs and ILs has been evidenced to be a breakthrough in chemistry and materials science due to their specific properties and applications [27-30]. The unique characteristics of both materials have let them to be useful in the field of electrode modification and electrochemistry [28-32]. It is reasonably proved that combination of CNTs and ILs can lead to create novel nanocomposites with improved multifunctional properties due to synergic effect of ILs and CNTs [34,35]. Additionally, the inherent interaction between ILs and CNTs produces a CNTs/ILs bulky gel with its conveniently applications. Consequently, more attentions are focused on the electrochemical sensors and bio-sensors based on CNTs/ILs nanocomposites [28-38].

On the other hand, sol-gel technology has received considerable attention to develop numerous chemical sensors, various chemical synthesizing and producing different solid materials. Sol-gel carbon composites are prepared simply by homogeneously dispersion of carbon powder in sol-gel matrices. These composites have several advantages such as high conductivity, wide operational voltage window in electrochemistry, relative chemical inertness, high mechanical stability, physical rigidity, being modified by chemical or biological compounds and stability in various solvents. In 1994, the sol-gel based carbon-ceramic electrode (CCE) was introduced by Lev and co-workers [39] who prepared this electrode through dispersion of carbon powder into the starting sol-gel solution; its surfaces can be regenerated *via* a simple polishing step and extensively applied for the designing of the electrochemical devices.

In the current work, by combining the advantages of CCE, multi-walled carbon nanotubes (MWCNTs) and IL, the MWCNTs/IL/CCE was designed by a simple, fast and repeatable procedure. Firstly, the surface characterisations, electrochemical properties and durability of the MWCNTs/IL/CCE were studied and then it was employed for the electrocatalytic oxidation and determination of Trp in the presence of uric acid (UA). The MWCNTs/IL/CCE exhibits considerable electrocatalytic activity in the oxidation of Trp due to its high surface area and synergic effect of IL and MWCNTs. Stability, electrocatalytic activities and electroanalytical applications of prepared modified electrode toward the determination of Trp were evaluated by different electrochemical techniques. Also its analytical performance for simultaneous determination of Trp in the presence of UA was evaluated.

EXPERIMENTAL

Chemicals

MWCNTs with 95% purity (10-20 nm diameters) and 1μm length was purchased from Nanolab (Brighton, MA 02135). Room temperature ionic liquid [1-ethyl-3-methyl imidazolium tetra fluoro borate] (EMI-BF4), methyltri-methoxysilane (MTMOS), tryptophan, uric acid and other chemicals were supplied by Merck or Fluka and used without any further purification. Phosphate buffer solutions,

0.1 M with different pH values were prepared from stock solutions of 0.1 M H_3PO_4, NaH_2PO_4, Na_2HPO_4 and NaOH. Double distilled water was used throughout the experiments.

Apparatus

An AUTOLAB PGSTAT-100 (potentiostat/galvanostat) equipped with a USB electrochemical interface and a GPES 4.9 software package (Eco Chemie, Netherlands) conjugated by a three-electrode system and a personal computer for data storage and processing was conducted for the electrochemical experiments. A three-electrode cell system includes a saturated calomel electrode (SCE) as the reference electrode, a platinum wire as the auxiliary electrode, and the nanocomposite modified electrode as the working electrode. Scanning electron microscopy (SEM) was carried out using a LEO 440i Oxford instrument.

Procedures

Preparation of the bare CCE. The bare carbon-ceramic electrode was prepared according to the procedure reported by Lev and co-workers [39] by mixing 0.15 ml MTMOS, 0.30 ml methanol and 10 μl hydrochloric acid (11 M). The obtained mixture was stirred for 2 min on magnetic stirrer, after that 0.3 g graphite powder was added and the resultant mixture was shaken for 1 min. A Teflon tube with length of 5 mm and inner diameter of 3-4 mm was filled with the prepared sol-gel carbon mixture, hand pressed and dried under ambient conditions (25 °C). In order to establish electrical contact a copper wire was inserted through the end of the working electrode.

Preparation of the CCE modified with MWCNTs/IL. For preparation of the carbon-ceramic electrode modified with MWCNTs/IL nanocomposite, firstly, 3.0 mg of MWCNTs and 6.0 μl of EMI-BF₄ were mixed using pestle and mortar for 15 min until a homogeneous black gel was obtained. After that, 0.1 mg MWCNTs/IL gel was transferred into an unfilled Teflon tube (3-4 mm inner diameter) to have a very thin gel film at the end of tube. Then, the sol-gel carbon mixture was transferred into the tube to fill the remaining empty part of the Teflon tube, hand pressed and dried under ambient conditions (25 °C). Finally, a copper wire was inserted into the end of the

electrode to establish electrical contact. The resulting modified electrode was referred as MWCNTs/IL/CCE.

RESULTS AND DISCUSSION

Characterization of MWCNTs/IL/CCE

To surface characterization the nanocomposite modified electrode, the SEM technique was utilized. The surface morphology of the bare CCE, MWCNTs/CCE and MWCNTs/IL/CCE is displayed in Fig. 1. It can be observed that the surface morphology of the bare CCE (Fig. 1A) is dense, scaly and has high sheet porosity. The SEM image of the same electrode after MWCNTs casting on the surface of CCE is shown in Fig. 1B. As seen, the MWCNTs film was uniformly spread on the electrode surface and they formed spaghetti-like and spiral structure. While, SEM image of MWCNTs/IL/CCE (image C) is different from image B and also image A. The MWCNTs are floated after being mixed with the IL, produce a uniform film and cover completely the surface of CCE.

For electrochemical characterization of the nanocomposite modified electrode, some effectible parameters such as electrocatalytic activity, electroactive real surface area, stability and reproducibility which are very important for a modified electrode are investigated. In the case of modified electrodes which do not have any intrinsically electrochemical behaviour in the absence of analyt, the reference compounds such as potassium hexacyanoferrate (III)/(II) system, $[Fe(CN)_6^{3-/4-}]$, was utilized for its electrochemical characterization. Figure 2A shows the cyclic voltammogram of the MWCNTs/IL/CCE in 5.0 mM potassium hexacyanoferrate in 0.1 M KCl. According to the obtained results, the MWCNTs/IL/CCE shows a well-defined redox anodic and cathodic peaks for the oxidation/reduction of $Fe(CN)_6^{3-/4-}$. The electroactive real surface area of the MWCNTs/IL/CCE was calculated by the obtained results from cyclic voltammetry based on the electrochemical behaviour of the $Fe(CN)_6^{3-/4-}$ solution regarding the Randles-Sevcik equation. The estimated electroactive surface area for the MWCNTs/IL/CCE is 1.85 cm^2, while the real surface areas for MWCNTs/CCE and bare CCE were 0.237 cm^2 and 0.162 cm^2, respectively [40]. The significant increase in the electroactive surface area
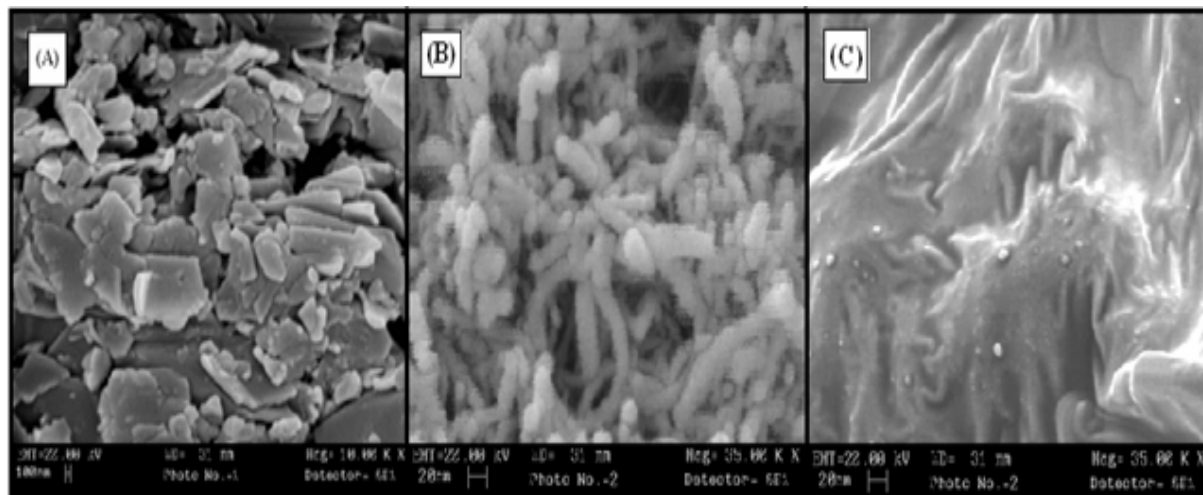
Fig. 1. Scanning electron micrograph of (A) bare CCE, (B) MWCNTs/CCE and (C) MWCNTs/IL/CCE.
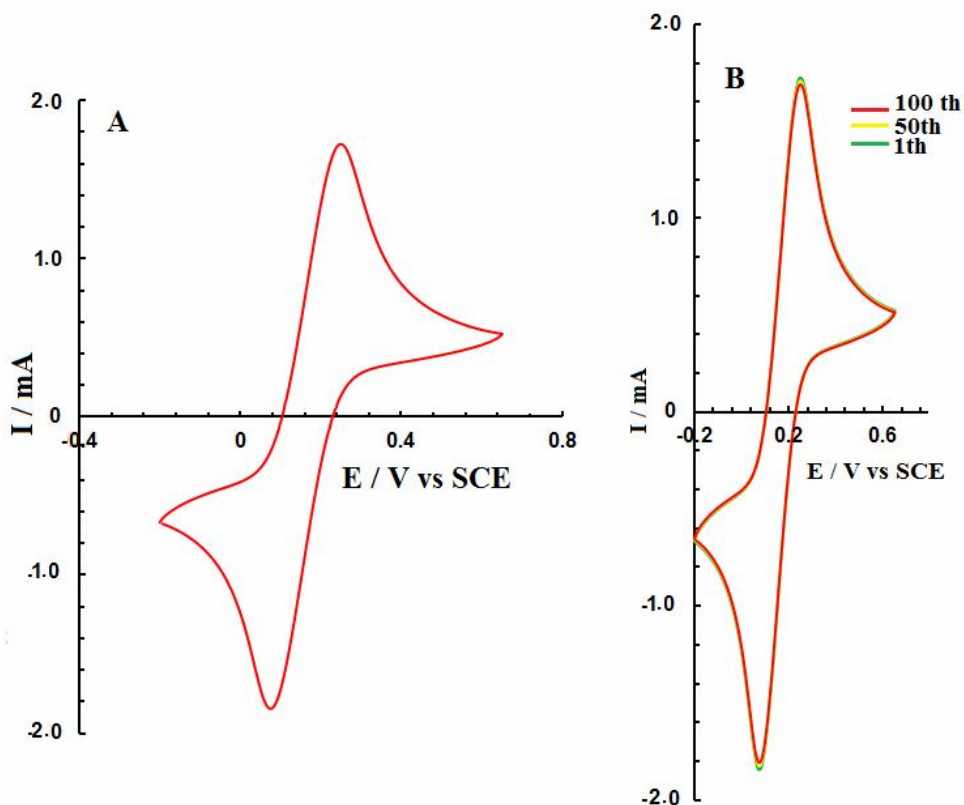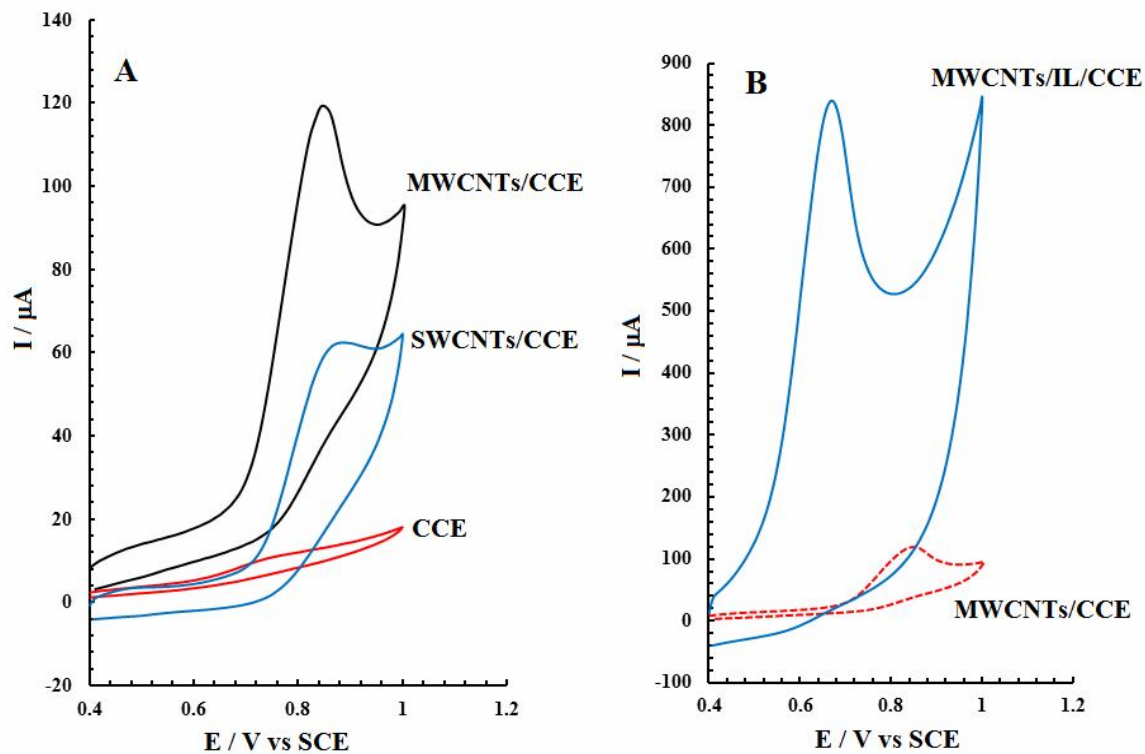

Fig. 2. (A) Cyclic voltammogram of 5.0×10^{-3} M potassium hexacyanoferrate (III)/(II) in 0.1M KCl on the MWCNTs/IL/CCE. (B) Cyclic voltammograms of same concentration of potassium hexacyanoferrate (III)/(II) on the MWCNTs/IL/CCE for the first, 50th and 100th scan. Scan rate: 50 mV s^{-1}.

Fig. 3. (A) Cyclic voltammograms of 1 mM Trp on the MWCNTs/CCE, SWCNTs/CCE and bare CCE
in phosphate buffer solution (pH = 7.0). (B) Cyclic voltammograms of same concentration of
Trp on the MWCNTs/CCE and MWCNTs/IL/CCE in the same conditions. Scan rate: 50 mV s^{-1}.
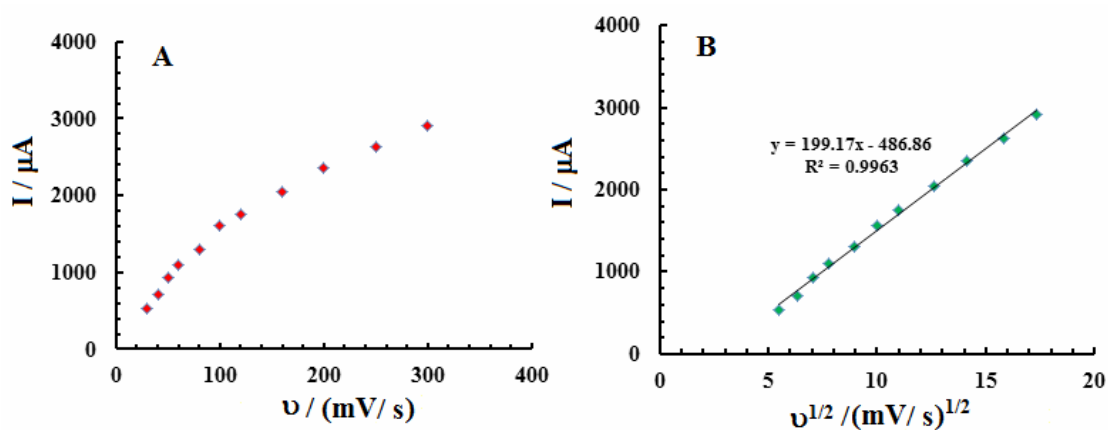
Fig. 4. (A) Plot of anodic peak currents *vs*. scan rate (υ) on different scan rates in the electrooxidation of 1 mM Trp
at the MWCNTs/IL/CCE. (B) Plots of anodic peak currents *vs*. square root of scan rate (υ$^{1/2}$).

offers that the MWCNTs/IL/CCE may be a promising candidate for electrochemical sensing. Furthermore, the stability and also the reproducibility of the modified electrode were investigated by cyclic voltammetry in the $Fe(CN)_6^{3-/4-}$ solution. Working stability of the prepared modified electrode was verified by evaluation of anodic and cathodic peak currents of $Fe(CN)_6^{3-/4-}$ after successive sweeps of several cyclic voltammograms (Fig. 2B). Concerning the obtained results, no considerable decrease in peak current was observed and peak current of 5.0 mM $Fe(CN)_6^{3-/4-}$ remaining on the MWCNTs/IL/CCE was almost 98% of its initial value after 100 cycles. Additionally, the electrolyte solution which was used for 100 repetitive cycles was replaced with fresh solution and no significant decrease was resulted. Also, the storage stability of the MWCNTs/IL nanocomposite modified electrode was investigated. For this purpose, the anodic and cathodic peak currents of $Fe(CN)_6^{3-/4-}$ on the nanocomposite modified electrode, which was kept at room temperature for more than 10 days in air, were compared with those of $Fe(CN)_6^{3-/4-}$ on the initial time of the same modified electrode. Practically, it was observed that the stored nanocomposite modified electrode has preserved 97% of its initial activity. Finally, to evaluate the reproducibility of the electrode preparation procedure, the cyclic voltammogram of $Fe(CN)_6^{3-/4-}$ solution with the concentration of 5.0 mM on the four independent MWCNTs/IL/CCEs were recorded. The RSD value of the obtained cathodic peak currents was about 1.7%.

Electrochemical behaviour of Trp at the MWCNTs/ IL/CCE. According to our previous reports, the CCEs modified with CNTs show electrocatalytic activity in the oxidation of some important biological compounds [41-45]. The electrocatalytic rule of the CNTs modifier leads to decrease of the anodic overpotential and enhance the anodic peak current in the electrooxidation processes. Figure 3A, shows the cyclic voltammetry responses of the bare CCE, SWCNTs/CCE and MWCNTs/CCE in the presence of 1 mM Trp in 0.1 M phosphate buffer solution (pH 7.0) at a scan rate of 50 mV s^{-1}. According to the obtained result, a relatively broad and very weak anodic peak was observed for the electrooxidation of Trp on the surface of the unmodified CCE. This observation revealed that the electrochemical oxidation of Trp on the bare CCE is sluggish with a slow electron transfer process. On the other hand, applying CNTs as modifier for electrode surface has led to a considerable enhancement in oxidation peak current of Trp. Moreover, using MWCNTs/CCE leads to achieve a well-defined and sharper anodic wave with lower peak potential for Trp in comparison with SWCNTs/CCE. This high electrocatalytic activity for the MWCNTs/CCE may be due to the unique properties of MWCNTs such as high specific surface area, subtle electronic properties and appropriate pore structures. Considering the benefits of MWCNTs and IL, the combination of MWCNTs and IL will be very promising. Therefore, it could be used to improve the performance of MWCNTs modified electrodes. As mentioned in the introduction, it is reasonably verified that hybridation of ILs and MWCNTs can offer a new composite materials with improved multifunctional properties. Figure 3B displays the cyclic voltammograms of Trp at the surface of MWCNTs/IL/CCE and MWCNTs/ CCE in 0.1 M phosphate buffer solution (pH 7.0) at a scan rate of 50 mV s^{-1}. As can be seen, the nanocomposite modified electrode has high electrocatalytic activity in comparison with alone MWCNTs modified electrode. Comparison of the cyclic voltammograms of Trp on the bare CCE, MWCNTs/CCE and MWCNTs/IL/CCE shows that the anodic peak potentials for electrooxidation of Trp are 840, 800 and 670 mV and the anodic peak currents are 10, 110 and 750 μA on the bare CCE, MWCNTs/CCE and MWCNTs/IL/CCE, respectively. On the other hand, compared with bare CCE and MWCNTs/CCE, the peak current on the MWCNTs/IL/CCE increased about 75 and 6.8 times, respectively, and the peak potential decreased about 170 mV and 130 mV, respectively to bare CCE and MWCNTs/CCE. These results may be ascribed by the following reasons: (I) MWCNTs particles usually are present as tangled bundles due to the strong intermolecular van der Waals interactions among the nanotubes which could lead to the formation of aggregates and reduction of specific area. Therefore, the MWCNTs film on the CCE obtained by drop coating is not uniform and only a part of the electrode surface may be covered by MWCNTs. When MWCNTs are ground and mixed with IL, the strong interaction between MWCNTs and IL eventually overcome MWCNTs intermolecular van der Waals interactions and detaches the MWCNTs from the bundles [26,46]. Thus,

more electroactive sites on MWCNTs can be exposed in the MWCNTs/IL/CCE, which can provide higher electroactive surface area. This surface increment was already proved by cyclic voltammogram of MWCNTs/IL/CCE in the presence of $Fe(CN)_6^{3-/4-}$ probe ions. (II) Moreover, these could be attributed to the synergistic effect of IL and MWCNTs. The ILs can extract many molecules, thus they can enhance the current response of analytes to a great extent [47,48]. On the other hand, the immidazolium-based ILs could interact with carbon nanotubes through π-π interaction, which detach the entangled MWCNTs bundles to form much finer bundles [26]. This is expected to improve the electrochemical catalysis properties of MWCNTs. Concerning all cyclic voltammograms in Fig. 3, it is clear that there is no reduction peak in the reverse scan, suggesting that the electrochemical reaction of Trp is a totally irreversible process at the bare CCE, MWCNTs/CCE and also at MWCNTs/IL/CCE [21-23,49-51].

The effect of scan rate on the electrochemical oxidation of Trp at the MWCNTs/IL/CCE was investigated and the obtained results are depicted in Fig. 4 (Fig. 4A shows the anodic peak current *vs.* scan rate and Fig. 4B shows the anodic peak current *vs.* square root of scan rate). It is obvious that the anodic peak current of Trp oxidation increased gradually when the scan rate was increased. The anodic peak currents were linearly proportional to the square root of scan rate in the ranges of 30-300 mV s^{-1}, suggests a typical diffusion-controlled electrochemical process [20-25]. The linear regression equations was expressed as $I_p/\mu A = 199.17\, \upsilon^{1/2} / (mV\, s^{-1})^{1/2} - 486.68$ with a correlation coefficient (R^2) of 0.996. Furthermore, the oxidation peak potential of Trp shifted toward more positive potential when the scan rate was increased which suggests a kinetic limitation in the reaction between nanocomposite modified electrode and Trp. Therefore, important information can be obtained about the rate determining step of the oxidation of Trp by estimation of the Tafel slope 'b'. For a totally irreversible diffusion controlled reaction, b can be calculated according to Eq. (1).

$$E_p = b/2\, \log\upsilon + constant \qquad (1)$$

Considering Eq. (1), the plot of E_p *vs.* $\log\upsilon$ leads to slope of b/2, where b is Tafel slope. According to the obtained

results, the Tafel slope of 242 mV have been calculated for the oxidation of Trp on the nanocomposite modified electrode indicating that electron transfer process is the rate limiting step. The charge transfer coefficient αn_α, where n_α is the number of electrons involved in the rate determining step, was calculated for the oxidation of Trp at the nanocomposite modified electrode by Eq. (2).

$$\alpha n_\alpha = 0.048\, (E_p - E_{p/2}) \qquad (2)$$

where E_p and $E_{p/2}$ are the anodic oxidation potential and anodic half-wave oxidation potential, respectively. Since Trp undergoes one electron oxidation at the rate determining step [49-51] the charge transfer coefficient α at the MWCNTs/IL/CCE is 0.52 which is in a good agreement with the reported results [22].

The primarily results revealed that the electrochemical behaviour of Trp is closely dependent on the pH of solution. Therefore, to investigate the electrooxidation mechanism, pH effect was investigated on the electrooxidation of Trp at the MWCNTs/IL/CCE in the pH ranges of 2.0-9.0. The effect of pH on the oxidation peak current and peak potential is displayed in Fig. 5. As can be seen, high acidic media leads to high performance of the electrooxidation of Trp and appearances of high anodic peak currents. While in low acidic media, the anodic peak current decreased and considerably stabilized and after a slight increase reached to maximum value at about pH = 7.0 and then decreased with increasing the pH (pH = 7.0-9.0) (Inset of A) [16,22]. In fact, Trp has two pK$_a$s; 2.38 and 9.39 which are related to carboxyl group and amino group, respectively. Therefore, Trp exists mainly as a neutral form [Indole group-CH$_2$-CH(COO$^-$)NH$_3^+$] in the solutions with pH in the ranges of 2.38-9.39, in the cationic form in the solutions with pH $\leq$ 2.38 and in the anionic form in the solutions with pH $\geq$ 9.39. Thus, the dependency of the oxidation anodic peak current of Trp *vs.* pH may be attributed to the influence of pH on the charge property and charge density of Trp [52]. Finally, as can be seen, the oxidation peak current reaches the maximum value at pH 7.0. Hence, the optimum pH; 7.0 (biological pH) is selected for Trp determination. Figure 5B displays the influence of pH value on the oxidation peak potential (E_p). It was found that E_p shifted toward less positive values by increasing the pH from 2.0 to 9.0. A
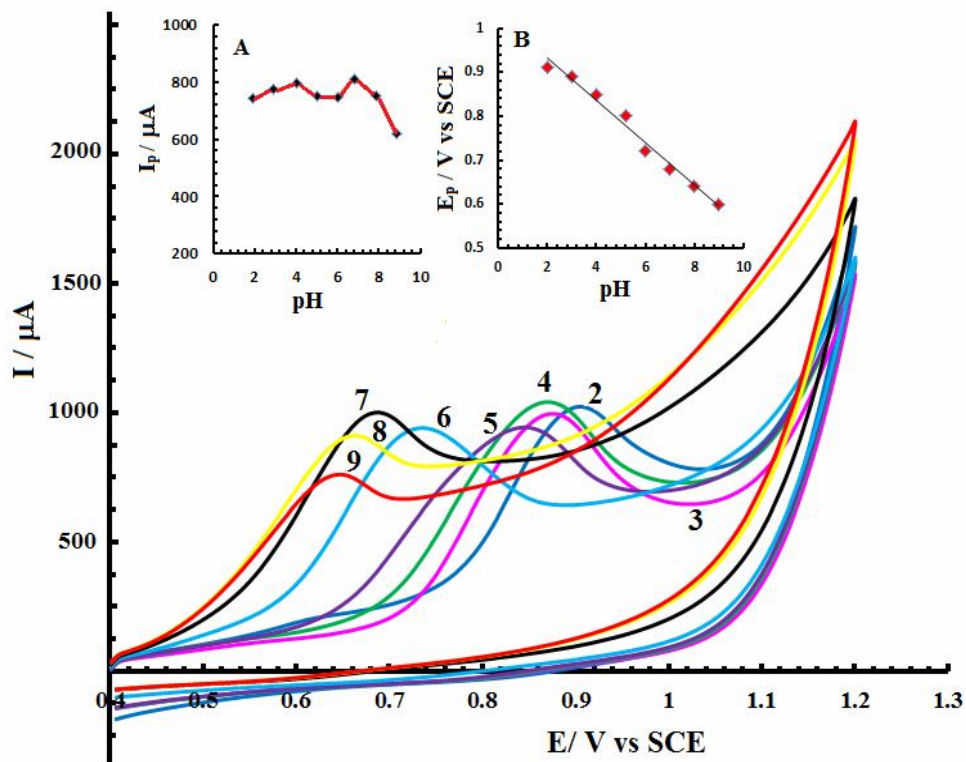
Fig. 5. Cyclic voltammograms of 1 mM Trp on the MWCNTs/IL/CCE in different pHs at scan rate of 50 mV s^{-1}. Inset A: plot of anodic peak currents *vs.* pH. Inset B: plot of anodic peak potentials *vs.* pH.
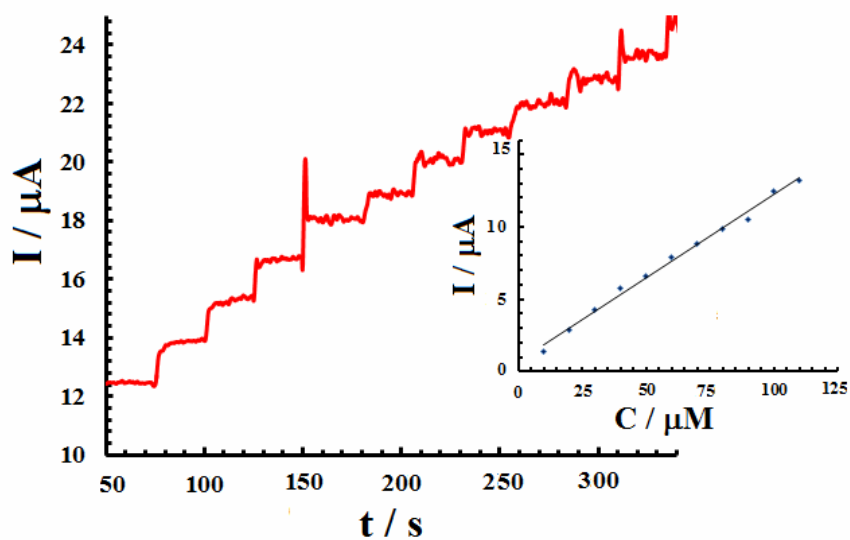
Fig. 6. Current-time recording to successive addition of 10 μM Trp at the MWCNTs/IL/CCE. Applied potential 0.73 V *vs.* SCE. Inset is the variation of currents *vs.* Trp concentrations.

162
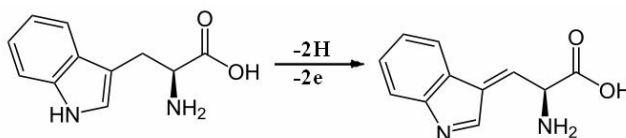
Scheme1. Electrooxidation of Trp at the modified electrodes such as MWCNTs/IL/CCE.

linear relationship can be constructed with following equation: $E_p = -0.054$ pH + 1.027, $R^2 = 0.996$. Taking into account of slope value of 0.054 V per pH unit [53], m/n value of 1 can be estimated, revealing that the proton-transfer number (m) is equal to the electron-transfer number (n). According to the results of above experiments and literature reports [17,23,54] the mechanism of Trp electro-oxidation reaction at the modified electrodes such as MWCNTs/IL/CCE can be proposed as shown in Scheme 1.

As can be seen, the electrochemical reaction mechanism of Trp at the MWCNTs/IL/CCE involves a two electron and two proton transfer in the electrode reaction process.

Determination of Trp

Under the selected experimental conditions, the analysis of Trp in the solution was conducted by cyclic voltammetric technique. A good linear relationship between the anodic peak current and the concentrations of Trp from 1×10^{-5} to 600×10^{-6} M was obtained by the cyclic voltammetric method. When the Trp concentration exceeded 600×10^{-6} M, the calibration curve began to leave the linear plot and detection limit was estimated to be 3×10^{-6} M (S/N = 3).

Taking into account of much higher current sensitivity of hydrodynamic amperometry and differential pulse voltammetry (DPV) in comparison with cyclic voltammetry, these techniques were employed to get the lower limit of detection. To obtain optimum conditions for amperometric determination of Trp under stirred condition, the hydrodynamic voltammograms of 1.5×10^{-2} M Trp at the MWCNTs/IL/CCE were recorded in the potential range of 0.10-0.9 V (the resulted data are not shown here). Accordingly, potential of 0.73 V *vs.* SCE was chosen as the working potential for amperometric determination of Trp under dynamic conditions. Figure 6 shows the typical steady-state catalytic current time response of the MWCNTs/IL/CCE in the presence of Trp at an applied potential of 0.73 V. As displayed, the well-defined responses were observed by addition of 1×10^{-6} M and $0.5 \times$

10^{-6} M of Trp, indicating stable and efficient electrocatalytic activity of the nanocomposite modified electrode. The linear calibration curve in the range of 1-125 $\times 10^{-6}$ M with a correlation coefficient of 0.9972 (inset of Fig. 6) was resulted, demonstrating that the regression line is well fitted with the experimental data and the regression equation can be applied in the determination of unknown sample. The detection limit (S/N = 3) was obtained to be 0.6×10^{-6} M.

In DPV method, in addition to higher current sensitivity, the charging current contribution to the background current is negligible. Applying this technique, a good linear relationship between anodic peak currents and Trp concentrations in the ranges 5×10^{-7}-7×10^{-5} M (Fig. 7 and its inset) resulted and detection limit was obtained to be 0.32×10^{-6} M. Therefore, as can be seen, compared to the obtained results for the cyclic voltammetry, hydrodynamic amperometry and DPV methods for the determination of Trp concentrations, the DPV method has wide linear dynamic ranges and low detection limit. For the reproducibility evaluation of the nanocomposite modified electrode, a 5.0×10^{-6} M Trp solution was measured with the same electrode in several times within a day by DPV method. The relative standard deviation *(*RSD*)* of the peak current was obtained to be 2.2% (n = 6), indicating that the nanocomposite modified electrode has good reproducibility. After several days of repetitive use, the response of the same modified electrode decreased only slightly. This result verified that the present nanocomposite modified electrode has high stability in Trp determination. Compared with other electrochemical methods [55-58] (Table 1), the present method has comparable linear dynamic range, limit of detection and RSD for the determination of Trp. Furthermore, the preparation of the present modified electrode is simple and convenient, and also the modified electrode is quite stable.

Interference Study

In order to investigate possible interferences in
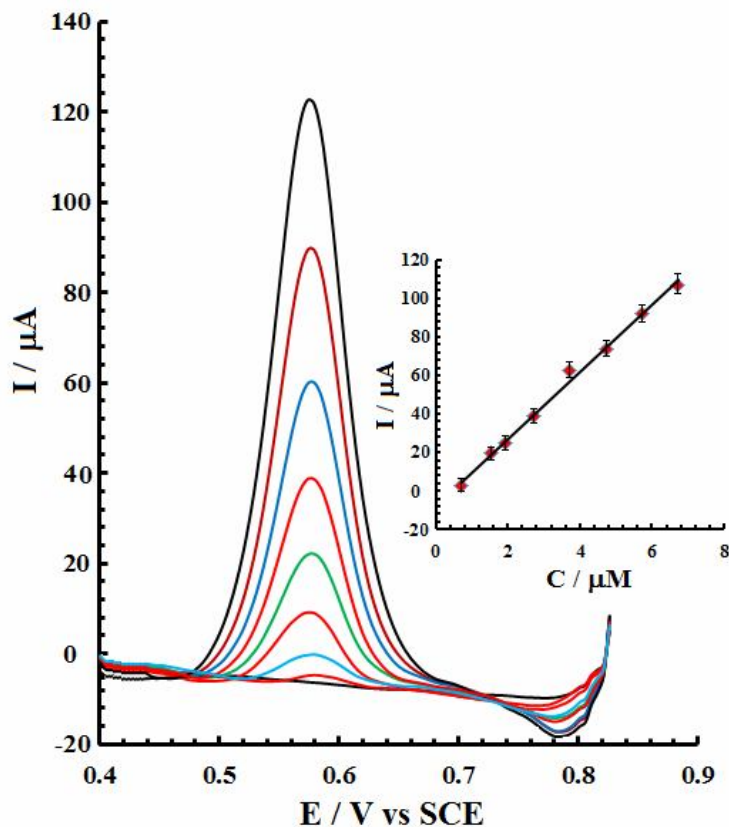
Fig. 7. DPVs of Trp at various concentrations: 0.5, 1.0, 1.8, 2.2, 3.0, 4.0, 5.0, 6.0 and 7.0 µM. Inset: Plot of anodic peak currents *vs*. Trp concentrations. Pulse amplitude: 70 mV. Pulse width: 50 ms.

determination of Trp at the MWCNTs/IL/CCE, various compounds and ions were added to 0.1 M phosphate buffer solution in the presence of 20×10^{-6} M Trp. For this propose, 10-fold concentration of interfering compounds and ions were added to the sample solution and the resulted error in Trp determination was calculated. If the tolerance limit was taken as the maximum concentration of the foreign species, which caused an approximately 5% relative error, no interference was observed. Considering this rule, possible interference of the common substances such as ascorbic acid (AA), acetaminophen (AC), Na^+, Cl^-, NO_3^-, Al^{3+}, and CO_3^{2-} on the Trp determination was evaluated. The obtained results are tabulated in Table 2. As can be seen, the present nanocomposite modified electrode has good selectivity toward determination of Trp and there is no considerable interference of investigated species.

Electrochemical Investigation of UA at the MWCNTs/IL/CCE

The electrochemical behaviour of UA was studied on the MWCNTs/IL/CCE and MWCNTs/CCE. According to the obtained results, higher anodic oxidation peak on the MWCNTs/IL/CCE was observed *vs*. MWCNTs/CCE and also bare CCE. Moreover, pH effect on the electrochemical behaviour of UA on the MWCNTs/IL/CCE was investigated (Fig. 8). As shown in inset A of Fig. 8, a decrease of anodic peak current was observed with increasing the pH value from 3.0 to 6.0, but after that up to pH 9.0 the peak current has remained almost constant. Therefore, the maximum stable anodic peak current was observed at pH value of 7.0. Also, it was found that peak potential is dependent on pH and that E_p shifted to less positive potentials with increasing the pH from 3.0 to 9.0. A linear relationship can be obtained with slope of 0.0696 V
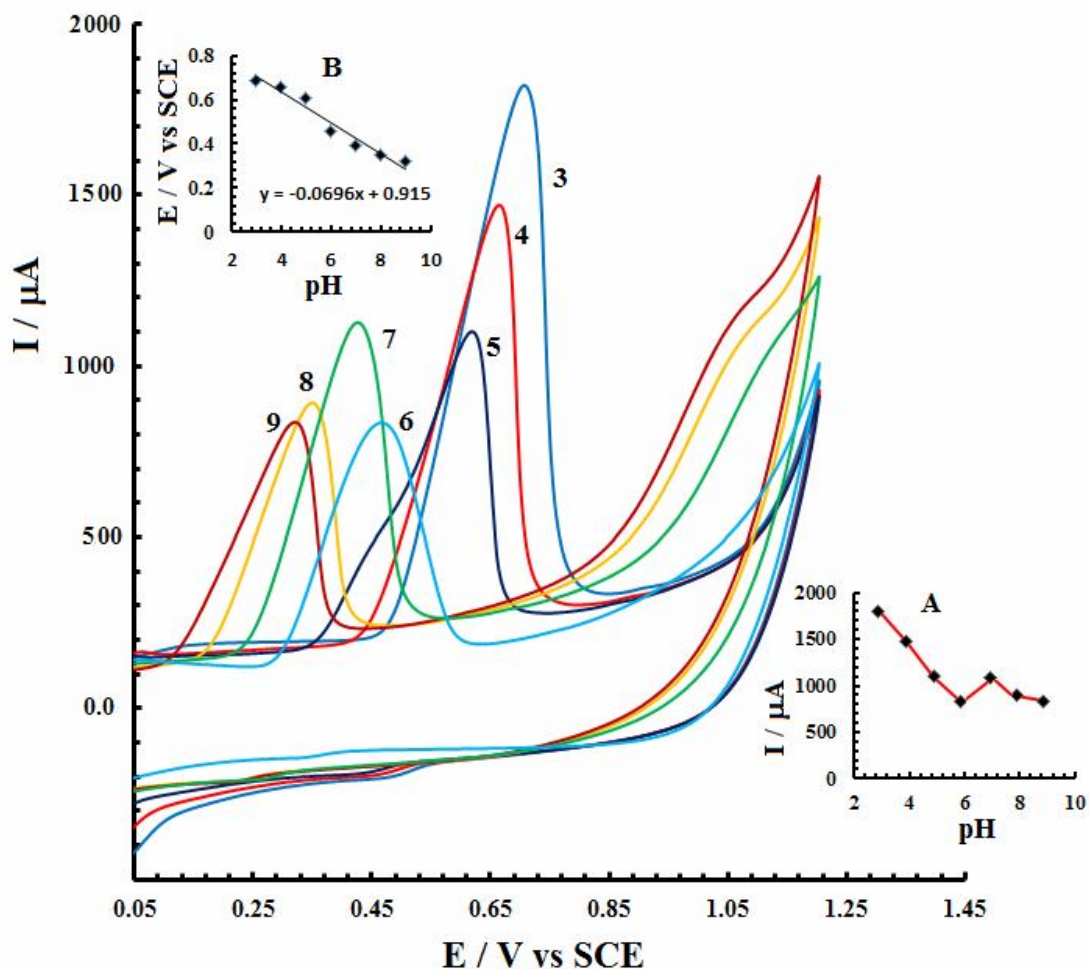
Fig. 8. pH effect on the electrochemical behaviour of UA on the MWCNTs/IL/CCE at scan rate of 50 mV s^{-1}. Inset A: plot of anodic peak potentials *vs.* pH and inset B: plot of anodic peak currents *vs.* pH.

per pH unit (inset B of Fig. 8) [53], from which m/n value of 1 is estimated, indicating that the proton-transfer number (m) is equal to the electron-transfer number (n). The effect of scan rate on the electrochemical oxidation of UA at the MWCNTs/IL/CCE was also investigated and the obtained result revealed that the anodic peak current is linearly proportional to the square root of scan rate in the range of 10-450 mV s^{-1}, suggesting a typical diffusion-controlled electrode process.

Electrochemical Investigation of Trp in the Presence of UA at the MWCNTs/IL/CCE

The cyclic voltammogram of Trp solution (0.5 × 10^{-4} M)

containing also the same concentration of UA was recorded at the MWCNTs/IL/CCE and the obtained result is depicted in Fig. 9A. As can be seen, the anodic peaks of Trp and UA in the forward scan are separated. Meanwhile, in order to obtain higher sensitivity and resolution the DPV was employed. Figure 9B shows the DPV obtained with the MWCNTs/IL/CCE in 1.8 × 10^{-6} M Trp solution containing same concentration of UA. The anodic peaks of Trp and UA are separated completely and the oxidation currents of Trp and UA can be detected simultaneously due to the nonoverlapping of their anodic peaks. It is worth recalling that the main purpose of the present study is the determination of Trp selectively and simultaneously in the

Table 1. Comparison of the Response Characteristics of Voltammetric Determination of Trp at Various Modified Electrodes

| No.	Modifier	Electrode	LOD (μM)	LDR (μM)	RSD (%)	Ref.
1	Gold nanoparticles/overoxidized-polyimidazole	GCE	0.7	3-34, 84-464	2.23	[16]
2	Ag@C core-shell nanocomposite	GCE	0.04	0.1-100	3.9	[17]
3	Ni(II)-ACDA modified gold nanoparticle	AuE	0.023	0.085-43.00	2.77-3.62	[22
4	Gold Nanoparticle	CILE	4	5 -900	-	[23]
5	Copper-cobalt hexacyanoferrate	GrE	6	10-900	-	[55]
6	Nano-TiO_2/ferrocene Carboxylic acid	CPE	0.124	0.4-14	-	[56]
7	Electrospun carbon nanofibers	CPE	0.1	0.1-119	1.0	[57]
8	Multi-walled carbon Nanotubes-cerium hexacyanoferrate	GCE	0.02	0.2-100	3.6	[58]
9	Multi-walled carbon Nanotubes / ionic liquid	CCE	0.32	0.5-70	2.2	This work

Table 2. Determination Errors (%) of Trp in the Presence of 10-Fold Concentration of Interfering Sspecies

Studied species	AC	AA	Na^+	Cl^-	NO_3^-	Al^{3+}	CO_3^{2-}
Trp determination error (%)	5	5	4	5	1	5	4

AA: Ascorbic acid and AC: Acetaminophen

presence of UA and *vice versa*. Consequently, the anodic signal of 1.8×10^{-6} M Trp at the MWCNTs/IL/CCE was carefully determined in the presence of increasing concentrations of UA (Fig. 10A). No significant change in the Trp oxidation currents was observed by changing the concentration of UA, while the anodic peak current of UA increased linearly with increasing its concentration (inset of Fig. 10A). Figure 10B shows the determination of Trp in the presence of UA. As can be seen from the inset of Fig. 10B,

the anodic peak currents of Trp increase linearly with increasing its concentration. These results revealed that MWCNTs/IL/CCE is highly suitable for the selective determination of Trp in a wide concentration ranges in the presence of various concentrations of UA and vice versa. Also, if the concentrations of Trp and UA are increased synchronously, the anodic peak currents of Trp and UA increase accordingly, as shown in Fig. 10C. It was also found that when the concentrations of both compounds
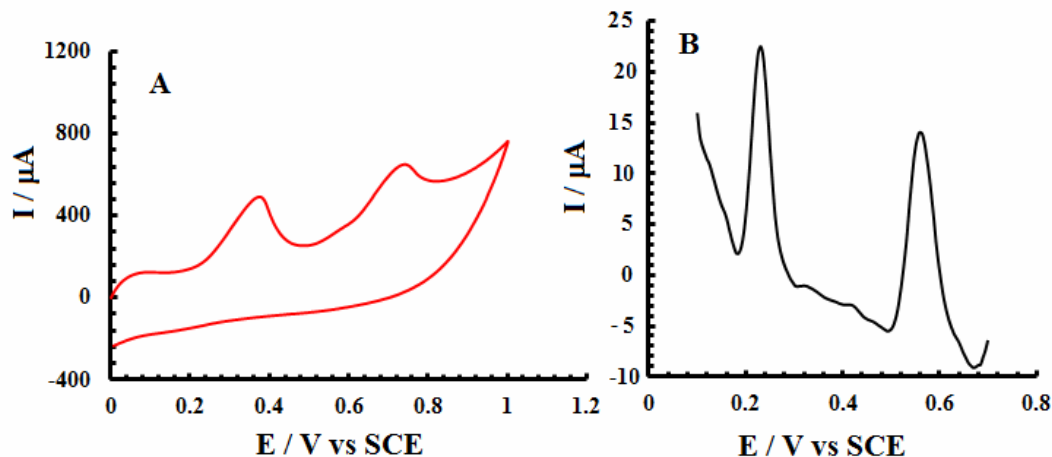
Fig. 9. (A) Cyclic voltammogram of Trp and UA on the MWCNTs/IL/CCE at concentration level of 0.5 mM, pH = 7.0 at scan rate of 50 mV s^{-1}. (B) DPV of Trp and UA on the MWCNTs/IL/CCE at concentration level of 1.8×10^{-6} M, pH = 7.0. Pulse amplitude: 70 mV. Pulse width: 50 ms.

increase simultaneously, both compounds exhibit oxidation peaks separately, without interfering each other. Thus, it can be concluded that the proposed method can be successfully applied for the simultaneous determination of Trp and UA at the optimum conditions by the DPV method.

Determination of Trp in Real Sample

As a practical application, the MWCNTs/IL modified electrode was also used to determination of Trp content in dough (a product of a milk factory in East Azarbaijan province, Iran). At first, 2 ml of dough was added to 10 ml phosphate buffer solution, and then a series of various volume of Trp standard solution was added. The DPV was applied for determination of Trp in prepared solutions (Fig. 10D). It was found that the DPV of the sample solution exhibited only one peak at about 0.55V (*vs*. SCE), which is associated with the oxidation of Trp. The concentration of Trp was calculated by standard addition, that the result was about 9.7×10^{-6} M. This suggests that the present modified electrode has some selectivity toward Trp in dough under the selected conditions.

CONCLUSIONS

A simple, fast, reproducible and convenient procedure

was used to fabrication of multi-walled carbon nanotubes/ionic liquid modified carbon-ceramic electrode, MWCNTs/IL/CCE. Application of a reversible electroactive couple, potassium hexacyanoferrate (III)/(II), as the electroactive probe compound revealed that MWCNTs/IL nanocomposite on CCE has a good chemical and electrochemical stability and it can be used as a chemically modified electrode to explore the electrocatalytic oxidation and determination of Trp. Trp that can be oxidized at MWCNTs/IL/CCE produced an anodic peak current at about 0.67 V (*vs*. SCE) in 0.1 M phosphate buffer solution (pH 7.0). This oxidation peak is suitable for the determination of Trp, and the peak current in different electrochemical methods is linear to its concentration over a certain range. Furthermore, the experimental results reported here have clearly indicated that Trp can be determined in the presence of UA and vice versa without any interference.

ACKNOWLEDGMENTS
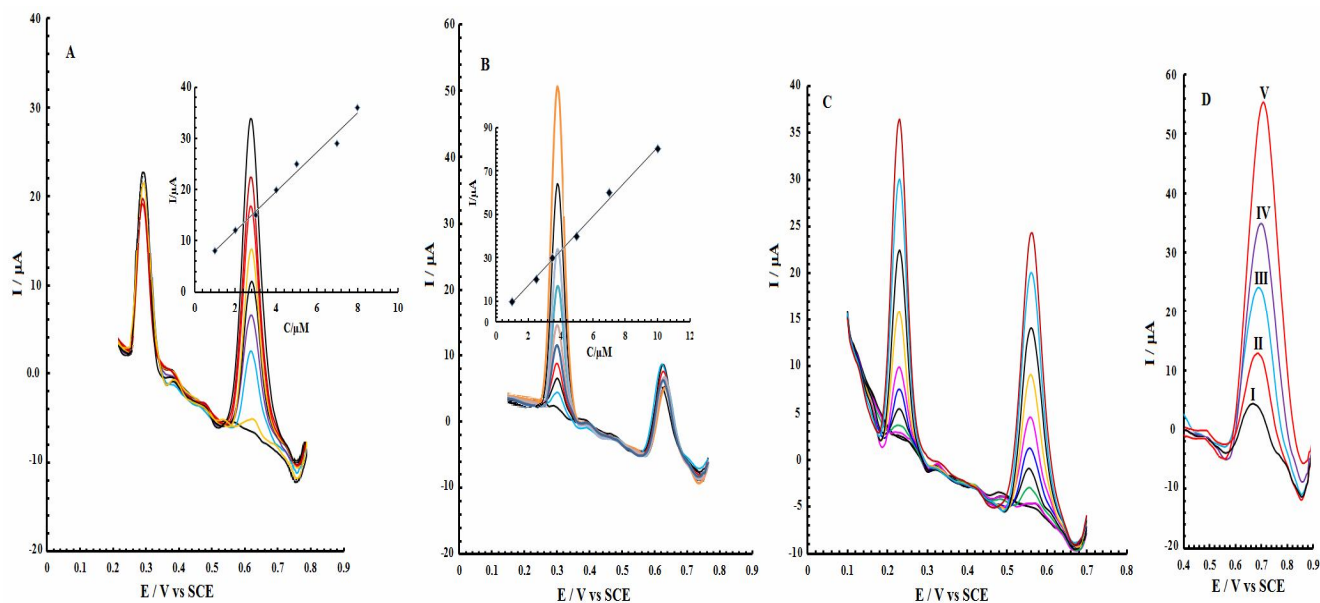
Fig. 10. (A) DPVs of Trp in the presence of UA at different concentrations, pH = 7.0, Inset: plot of anodic peak currents *vs*. UA concentrations. (B) DPVs of UA in the presence of Trp at different concentrations, pH = 7.0, Inset: plot of anodic peak currents *vs*. Trp concentrations. (C) DPVs of different concentrations of Trp and UA in the same solution. (D) DPV of Trp in real sample solution (I) and increasing concentration of standard Trp solutions (II-V). Pulse amplitude: 70 mV. Pulse width: 50 ms.

REFERENCES

[1] M.H. Fernstrom, J.D. Fernstrom, Life Sci. 57 (1995) PL97.

[2] W. Lian, D.J. Ma, X.U. Xu, Y. Chen, Y.L. Wu, J. Digest. Dis. 13 (2012) 100.

[3] M.E. Soto, A.M. Ares, J. Bernal, M.J. Nozal, J.L. Bernal, J. Chromatogr. A 1218 (2011) 7592.

[4] J. Galba, A. Michalicova, V. Parrak, M. Novak, A. Kovac, J. Pharmaceut. Biomed. Anal. 117 (2016) 85.

[5] A. Zinellu, S. Sotgia, L. Deiana, G. Talanas, P. Terrosu, C. Carru, J. Sep. Sci. 35 (2012) 1146.

[6] Y. Takagai, S. Igarashi, Chem. Pharm. Bull. 51 (2003) 373.

[7] M. Zhao, M.-F. Zhou, H. Feng, X.-X. Cong, X.-L. Wang, Chromatographia 79 (2016) 911.

[8] A.J. Lewis, P.J. Holden, R.C. Ewan, D.R. Zimmerman, J. Agricultural and Food Chem. 24 (1976) 1081.

[9] T. Sasaki, B. Abrams, B.L. Horecker, Anal. Biochem.

65 (1975) 396.

[10] Y. Wu, S. Han, Anal. Chem.: An Indian J. 16 (2016) 1.

[11] H. Qiu, C. Luo, M. Sun, F. Lu, L. Fan, X. Li, Talanta 98 (2012) 226.

[12] F. Wu, B. Tong, Q. Zhang, Anal. Sci. 27 (2011) 529.

[13] C.-J. Lee, J. Yang, Anal. Biochem. 359 (2006) 124.

[14] M.M. Yust, J. Pedroche, J. Girón-Calle, J. Vioque, F. Millán, M. Alaiz, Food Chem. 85 (2004) 317.

[15] A. Babaei, M. Zendehdel, B. Khalilzadeh, A. Taheri, Colloid Surface B: Biointerfaces 66 (2008) 226.

[16] C. Wang, R. Yuan, Y. Chai, S. Chen, F. Hu, M. Zhang, Anal. Chim. Acta 741 (2012) 15.

[17] S. Mao, W. Li, Y. Long, Y. Tu, A. Deng, Anal. Chim. Acta 738 (2012) 35.

[18] S.M. Ghoreishi, M. Behpour, F. Saeidinejad, Anal. Methods 4 (2012) 2447.

[19] H. Beitollahi, A. Mohadesi, S.K. Mahani, H.K. Maleh, A. Akbari, Turk. J. Chem. 36 (2012) 526.

[20] K.-Q. Deng, J.-h. Zhou, X.-F. Li, Colloid Surface B:

Biointerfaces 101 (2012) 183.

[21] W. Li, C. Li, Y. Kuang, P. Deng, S. Zhang, J. Xu, Microchim. Acta 176 (2012) 455.

[22] M.B. Gholivand, A. Pashabadi, A. Azadbakht, S. Menati, Electrochim. Acta 56 (2011) 4022.

[23] A. Safavi, S. Momeni, Electroanalysis 22 (2010) 2848.

[24] Q. Sheng, R. Liu, H. Zhang, J. Zheng, J. Iran. Chem. Soc. 13 (2016) 1189.

[25] M. Mazloum-Ardakani, Z. Taleat, H. Beitollahi, H. Naeimi, J. Iran. Chem. Soc. 7 (2010) 251.

[26] B.K. Price, J.L. Hudson, J.M. Tour, J. Am. Chem. Soc. 127 (2005) 14867.

[27] R.T. Kachoosangi, M.M. Musameh, I. Abu-Yousef, J. M. Yousef, S.M. Kanan, L. Xiao, S.G. Davies, A. Russell, R.G. Compton, Anal. Chem. 81 (2008) 435.

[28] M. Rahimi-Nasrabadi, A. Khoshroo, M. Mazloum-Ardakani, Sensor Actuat. B: Chem. 240 (2017) 125.

[29] F. Jalali, M. Ardeshiri, Mater. Sci. Engin. C 69 (2016) 276.

[30] M. Fouladgar, Sensor Actuat. B: Chem. 230 (2016) 456.

[31] S. Cheraghi, M.A. Taher, J. Mol. Liquids 219 (2016) 1023.

[32] H. Rajabi, M. Noroozifar, M. Khorasani-Motlagh, Anal. Bioanal. Electrochem. 8 (2016) 522.

[33] T. Fukushima, A. Kosaka, Y. Ishimura, T. Yamamoto, T. Takigawa, N. Ishii, T. Aida, Science 300 (2003) 2072.

[34] M.R. Majidi, M.H. Pournaghi-Azar, R. Fadakar Bajeh Baj, A. Naseri, Int. J. Environ. Anal. Chem. 96 (2016) 50.

[35] R. Faramarzi, A.R Taheri, M. Roushani, Anal. Bioanal. Electrochem. 7 (2015) 666.

[36] N. Nasirizadeh, Z. Shekari, M. Dehghani, S. Makarem, J. Food Drug Anal. 24 (2016) 406.

[37] S.M. Ghoreishi, M. Behpour, S. Mousavi, A. Khoobi, F.S. Ghoreishi, Anal. Methods 7 (2015) 466.

[38] B. Jahanshahi, J. Raoof, M. Amiri-Aref, R. Ojani, J. Chilean Chem. Soc. 59 (2015) 2692.

[39] O. Lev, Z. Wu, S. Bharathi, V. Glezer, A. Modestov, J. Gun, L. Rabinovich, S. Sampath, Chem. Mater. 9 (1997) 2354.

[40] B. Habibi, M. Jahanbakhshi, M.H. Pournaghi-Azar, Microchim. Acta 177 (2011) 185.

[41] B. Habibi, M. Abazari, M.H. Pournaghi-Azar, Colloid Surface B: Biointerfaces 114 (2014) 89.

[42] B. Habibi, M. Jahanbakhshi, M. Abazari, J. Iran. Chem. Soc. 11 (2014) 511.

[43] B. Habibi, M. Jahanbakhshi, Electrochim. Acta 118 (2014) 10.

[44] B. Habibi, M.H. Pournaghi-Azar, Electrochim. Acta 55 (2010) 5492.

[45] B. Habibi, M. Jahanbakhshi, M.H. Pournaghi-Azar, Electrochim. Acta 56 (2011) 2888.

[46] X. Liu, Z. Ding, Y. He, Z. Xue, X. Zhao, X. Lu, Colloid Surface B: Biointerfaces 79 (2010) 27.

[47] H. Liu, P. He, Z. Li, C. Sun, L. Shi, Y. Liu, G. Zhu, J. Li, Electrochem. Commun. 7 (2005) 1357.

[48] L.I.N. Tomé, V.T.R. Catambas, A.R.R. Teles, M.G. Freire, I.M. Marrucho, J.O.A.P. Coutinho, Sep. Purif. Technol. 72 (2010) 167.

[49] S. Shahrokhian, L. Fotouhi, Sensor Actuat. B: Chem. 123 (2007) 942.

[50] J. Li, D. Kuang, Y. Feng, F. Zhang, Z. Xu, M. Liu, D. Wang, Biosens. Bioelectron. 42 (2013) 198.

[51] W. Huang, G. Mai, Y. Liu, C. Yang, W. Qua, J. Nanosci. Nanotechnol. 4 (2004) 423.

[52] X. Liu, L. Luo, Y. Ding, D. Ye, Bioelectrochemistry 82 (2011) 38.

[53] K.-J. Huang, C.-X. Xu, J.-Y. Sun, W.-Z. Xie, L. Peng, Anal. Lett. 43 (2009) 176.

[54] Y. Guo, S. Guo, Y. Fang, S. Dong, Electrochim. Acta 55 (2010) 3927.

[55] Y. Liu, L. Xu, Sensors 7 (2007) 2446.

[56] J.-B. Raoof, R. Ojani, M. Baghayeri, Sensor Actuat. B: Chem. 143 (2009) 261.

[57] X. Tang, Y. Liu, H. Hou, T. You, Talanta 80 (2010) 2182.

[58] B. Fang, Y. Wei, M. Li, G. Wang, W. Zhang, Talanta 72 (2007) 1302.